ELSEVIER

Surface Science 347 (1996) 289–302

surface science

Sites for arsine adsorption on GaAs(001)

Haihua Qi, Paul E. Gee, Robert F. Hicks *

Chemical Engineering Department, University of California, Los Angeles, CA 90095-1592, USA

Received 5 May 1995; accepted for publication 26 September 1995

Abstract

Arsine adsorption on c(2×8) and (1×6) GaAs(001) at 303–573 K has been studied by internal-reflection infrared spectroscopy. We have discovered that arsine adsorbs onto two sites: second-layer Ga atoms and Ga dimers. On the c(2×8), arsine dissociatively adsorbs on second-layer Ga atoms, forming arsenic monohydrides and transferring two H atoms each to nearby As dimers. On the (1×6), arsine dissociatively adsorbs on Ga dimers, and also transfers H atoms to As sites. The saturation coverage of arsine at 303 K on the (1×6) is twice that on the c(2×8). Also, more As-H infrared bands are observed, indicating that several AsH_x species are formed. Dosing the surfaces with arsine at successively higher temperatures from 303 to 473 K leads to the loss of adsorbed AsH_x species. At 573 K, no change in the c(2×8) occurs upon extended exposure to arsine. However, on the (1×6), the Ga dimers are replaced by As dimers during arsine dosing, and at 573 K, 1800 L of AsH_3 is sufficient to convert the (1×6) into the c(2×8) reconstruction. We conclude that during vapor-phase epitaxy of GaAs with trimethylgallium and arsine, AsH_3 decomposes on second-layer Ga atoms and Ga dimers. However, on the latter sites the arsenic is more likely to incorporate into the crystal, instead of desorbing as As_2 or As_4.

Keywords: Chemical vapor deposition; Chemisorption; Epitaxy; Gallium arsenide; Infrared absorption spectroscopy; Models of surface chemical reactions; Reflection spectroscopy; Single crystal surfaces; Vibrations of adsorbed molecules

1. Introduction

Arsine (AsH_3) is the preferred group V source for the organometallic vapor-phase epitaxy (OMVPE) of compound semiconductors [1–7]. Arsine is fed in large excess over the amount of trimethylgallium and other group III sources fed to the reactor. Typically, V/III mole ratios of ten or more are used [1,2,6,7]. The excess arsine is required to keep the surface in an arsenic-rich condition during growth. On gallium-rich surfaces, the methyl groups from trimethylgallium decompose into carbon, which dopes the semiconductor film in an undesirable way [4,8,9]. At high V/III ratios, very little arsine is utilized in the film, such that most of the chemical passes through the reactor and is discarded. In order to develop new strategies that utilize arsine more efficiently, it is essential that we understand how this molecule decomposes during GaAs OMVPE.

The mechanism of arsine decomposition has been studied by several researchers [3,10–16]. White and coworkers [13,14] found that arsine dissociatively adsorbs onto GaAs(001) at temperatures greater than 140 K. Upon heating the crystal, most of the adsorbed arsine recombines and desorbs, while a small fraction irreversibly decomposes by desorbing hydrogen. Bansenauer and Creighton [16] found that on the c(2×8) and (4×6) surfaces, the amount of arsine decomposing

*Corresponding author. Fax: +1 310 206 4107.

SSDI 0039-6028(95)00982-5

during thermal desorption equalled approximately 0.01 ML (where 1.0 ML = 1 atom per (1×1) unit cell $= 6.26\times10^{14}$ atoms/cm^2). These authors also exposed GaAs(001) to 10^4–10^6 L of arsine at 373–623 K (1 L $= 10^{-6}$ Torr·s), and observed the deposition of up to 1.7 ML of As atoms. When they heated the crystal above 623 K, the arsenic desorbed as As_4 and As_2, and converted the surface back into a gallium-rich reconstruction. Arsenic desorption between 673 and 873 K has also been observed in studies of GaAs(001) surfaces that have been prepared by molecular-beam epitaxy (MBE) [17–20]. Based on this prior work, we conclude that arsine may decompose in three different ways during GaAs OMVPE:

$$AsH_3 + Ga_s \rightarrow GaAs_s + \tfrac{3}{2}H_2, \quad (1)$$

$$2AsH_3 \rightarrow As_2 + 3H_2, \quad (2)$$

$$4AsH_3 \rightarrow As_4 + 6H_2, \quad (3)$$

where the subscript s refers to the surface of the crystal. Only the first reaction leads to film growth. The latter two produce gas-phase As_2 and As_4 which must be transported out of the reactor and disposed of. How efficiently arsine is used in the OMVPE process is determined by the rate of reaction (1) relative to the rates of reactions (2) and (3).

Since reactions (1)–(3) all occur on the surface of gallium arsenide, it may be presumed that different sites promote the formation of one product over the other two. For example, Banse and Creighton [15] observed As_4 desorption at As coverages greater than one monolayer, whereas As_2 desorbed from surfaces with lower As coverages. This suggests that the selectivity for arsine decomposition into GaAs depends on the composition of the surface during growth. Thus it is important to identify the sites on GaAs(001) that are involved in each of the reactions listed above.

The surface structure of GaAs(001) has been characterized through theoretical calculations and experimentally by low-energy electron diffraction (LEED), X-ray photoemission spectroscopy (XPS), and scanning tunneling microscopy (STM) [17–25]. These studies have shown that the arsenic and gallium atoms in the top layer form dimers [26]. The As dimers are oriented parallel to the $[\bar{1}10]$ axis, while the Ga dimers are parallel to the [110] axis. The distribution of As and Ga dimers in the top layer depends on the As coverage. Shown in Fig. 1 are ball-and-stick models for three reconstructions of GaAs(001). At an As coverage of 0.75, the surface reconstructs into a $\beta(2\times4)$ or a $\beta2(2\times4)$ phase, both of which contain three As dimers per unit cell. The actual LEED pattern for these structures is $c(2\times8)$, because adjacent cells in the $[\bar{1}10]$ direction are staggered with respect to each other [22]. By contrast, at an As coverage of 0.5, a (2×6) structure is formed which contains two As dimers and two Ga dimers. Disorder between adjacent rows of dimers leads to a (1×6) LEED pattern for this surface [19].

We have found that there are four principle adsorption sites on GaAs(001) [27,28]: As dimers,

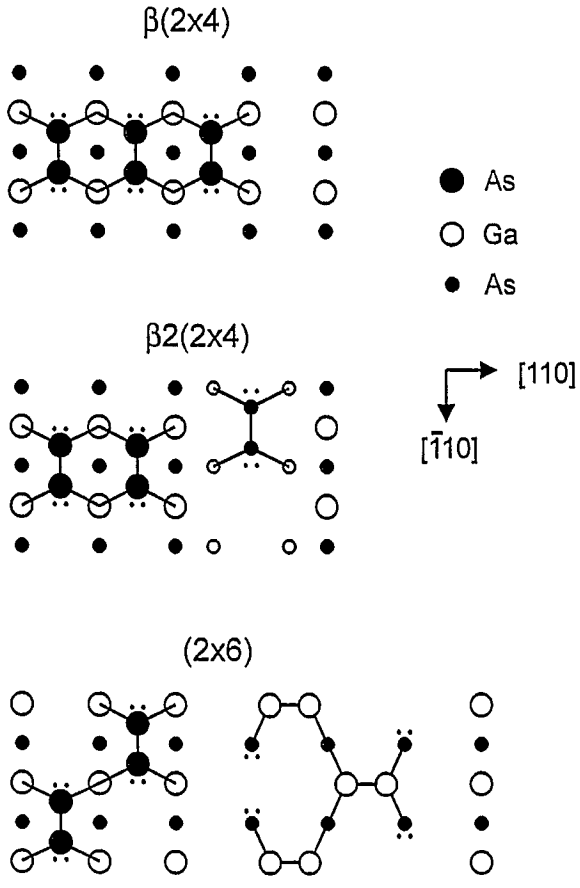

Fig. 1. Ball-and-stick models for the $\beta(2\times4)$, $\beta2(2\times4)$, and (2×6) reconstructions of GaAs(001) (after Refs. [19] and [25]).

Ga dimers, second-layer As atoms, and second-layer Ga atoms. The second-layer atoms are the threefold coordinated atoms that are exposed at dimer vacancies, at steps, and at the boundaries between regions terminated with different dimers. These four sites have been identified by adsorbing hydrogen atoms on the $c(2\times8)$ and (1×6) reconstructions, and then recording the vibrational spectra of the resultant As and Ga hydrides. Different hydride bonds are made to the four adsorption sites, and these can be distinguished from each other by the frequencies of their stretching vibrations. Referring to Fig. 1, it is seen that there are two adsorption sites on the (2×4) surfaces, As dimers and second-layer Ga atoms, whereas all four sites are present on the (2×6) surface. This difference in the distribution of sites is borne out by the infrared spectra of adsorbed hydrogen [28]. Having identified these sites, we have begun to study the adsorption of other molecules on GaAs(001), such as trimethylgallium [29] and arsine.

In this paper, we present the results of an infrared study of arsine adsorption on $c(2\times8)$ and (1×6) GaAs(001). The hydrides detected in the infrared spectra during dosing at different temperatures reveal the decomposition pathway for arsine. Hydrogen titration before and after arsine decomposition has been used to detect changes in the surface composition, and in this way, determine whether the arsenic is incorporated (reaction (1)), or desorbed (reaction (2)). These data also indicate on which sites these reactions occur. Based on this information and other published results, we present a mechanism for arsine decomposition on GaAs(001) that explicitly includes the surface sites. We show that arsine adsorbs and decomposes on Ga dimers and on second-layer Ga atoms, but that only on the former sites is the arsenic incorporated into the crystal lattice.

2. Experimental methods

The experiments were conducted in an ultrahigh vacuum chamber equipped with a PHI 5000 XPS spectrometer, a Princeton Instruments reverse-view LEED, and a Digilab FTS-40 infrared spectrometer. The infrared spectra were acquired by multiple internal reflection through an undoped single crystal of GaAs(001) (Marubeni America, $R=2\times10^{7}$ Ω cm). The crystal was cut into a trapezoid 50 mm long $\times$ 10 mm wide $\times$ 0.64 mm thick with 45° bevels at each end. The long axis of the crystal was parallel to the [110] direction. The infrared beam was focussed onto the beveled edge of the crystal with a CaF_2 lens. After exiting the sample, the IR beam was refocussed with a mirror onto an Infrared Associates MCT detector. The CaF_2 lens and the CaF_2 chamber windows prevented the transmission of light with frequencies below 1000 cm^{-1}.

The GaAs(001) crystal was cleaned in acetone and methanol, etched in (1:1:10) H_3PO_4:H_2O_2:H_2O solution for 15 s, rinsed in deionized water, etched in (1:1) HCl:H_2O solution for 5 min, and rinsed again in water. Then the sample was mounted onto a molybdenum holder, transferred into the chamber, and heated to 853 K for 1 min. No oxygen or carbon was detected by XPS after heating. The $c(2\times8)$ surface was produced by exposing the crystal to 1.5×10^{-7} Torr of AsH_3 at 573 K for 15 min, followed by heating in vacuum at 573 K for another 10 min. The (1×6) was obtained by exposing the crystal to an effusive beam of trimethylgallium (TMGa) at 2.3×10^{11} molecules/cm^2 s at 573 K for 20 min, then annealing it at 853 K for 1 min [29]. After each treatment, the sample was cooled and a LEED pattern and an XPS spectrum were taken. At a photoelectron escape angle of 45°, the ratios of As/Ga $2p_{3/2}$ peak areas in the XPS spectrum were 1.6 and 1.3 for the $c(2\times8)$ and the (1×6) surfaces, respectively, and were assumed to correspond to As coverages of 0.75 and 0.50.

Arsine was adsorbed onto the GaAs(001) sample by introducing 5×10^{-7} Torr of AsH_3 into the chamber for periods of up to 1 h. During arsine dosing, the sample was held at temperatures between 303 and 573 K. Hydrogen was adsorbed onto the crystal at 303 K by dissociating H_2 molecules over a white-hot, tungsten filament located 4 cm above the sample face. Saturation uptake of hydrogen was achieved after a 40-min exposure using a background pressure of 5×10^{-7} Torr of H_2. The impingement rate of the H atoms was

estimated to be 0.1% of that of the H_2 molecules [28].

After adsorbing arsine to a saturation coverage at 303 K, XPS spectra were recorded. The As/Ga $2p\frac{3}{2}$ area ratios increased from 1.60 to 1.68 for the $c(2\times8)$ and from 1.30 to 1.36 for the (1×6). Infrared reflectance spectra were recorded before and during arsine and hydrogen adsorption, and were acquired by signal averaging 512 scans at 8 cm^{-1} resolution. The changes in reflectance spectra shown in this paper are reported on a per reflection basis. They were obtained by taking the ratio of the spectrum collected during adsorption to that collected beforehand, and then dividing the result by the number of reflections off the front face of the crystal, $n_R = 38$.

Two difficulties were encountered in acquiring representative spectra for arsine adsorption on GaAs(001). First, the arsine was dissociated by any filaments turned on inside the chamber, such as the ion gauge or the X-ray source. The arsine fragments adsorbed onto the crystal and increased the uptake beyond that due to the molecules alone. This problem was avoided by keeping all the filaments off during arsine dosing. The second problem encountered was arsine adsorption on the back face of the crystal. In order to prevent absorption of the internally reflected light by the molybdenum plate, a groove, 0.15 mm deep × 8 mm wide, was cut out of the metal behind the GaAs crystal. This thin space provided arsine with access to the back face. The condition of the opposite side of the crystal was not certain throughout the experiments. While it received similar exposures to temperature and arsine pressure, it could not be dosed with the effusive beam of TMGa. This problem was overcome by titrating the surface with deuterium (D) atoms after arsine adsorption. The D atoms displaced the hydrides associated with the adsorbed arsine on the front face of the crystal. This occurred either by H/D exchange, or by displacement of the adsorbed AsH_3 by D. Since the D atoms cannot survive collisions with metal surfaces, they were unable to displace the hydrides present on the back face of the crystal. By rationing the spectra obtained after deuterium titration to that obtained after arsine adsorption, the hydrides due to the adsorbed arsine appeared as negative peaks in the reflectance spectrum.

3. Results

3.1. Arsine adsorption at 303 K

Shown in Fig. 2a are polarized reflectance spectra for a saturation coverage of arsine on $c(2\times8)$ GaAs(001) at 303 K. The inset diagram shows the orientation of the electric fields with respect to the crystal axis. The s-polarized spectrum contains three sharp peaks at 2165, 2140, and 2080 cm^{-1}, which are superimposed on a broad band extending from 2150 to 1950 cm^{-1}. Conversely, the p-polarized spectrum contains the broad band, but no sharp peaks. Presented in Fig. 2b is the unpolarized reflectance spectrum for adsorbed arsine on the $c(2\times8)$. This spectrum is

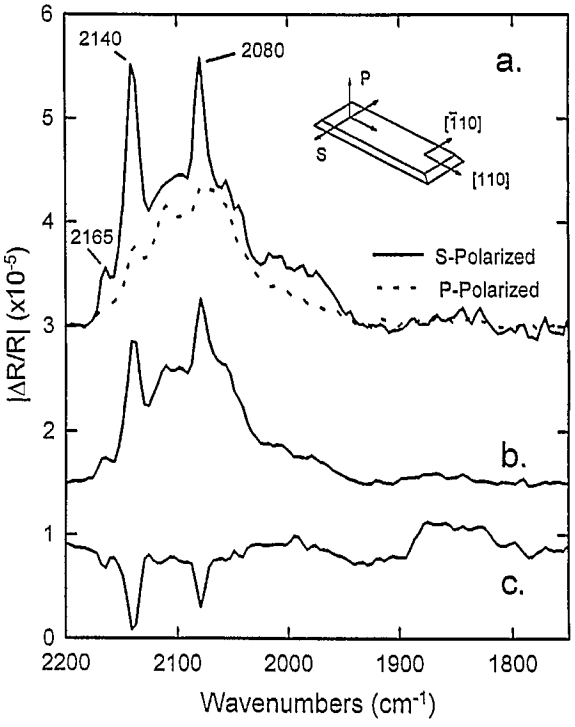

Fig. 2. Infrared reflectance spectra of adsorbed arsine on $c(2\times8)$ GaAs(001) at 303 K: (a) s- and p-polarized spectra (inset diagram reveals crystal orientation); (b) unpolarized spectrum; and (c) unpolarized spectrum after deuterium titration of the adsorbed arsine.

identical to the s-polarized spectrum, except that the overall intensity is reduced by 50%. In Fig. 2c, an unpolarized reflectance spectrum is shown for deuterium titration of the adsorbed arsine. Negative peaks are recorded of the adsorbed hydrides that are displaced by the D atoms. This spectrum contains only the three sharp peaks at 2165, 2140 and 2080 cm^{-1}, indicating that they are due to arsine adsorption on the c(2×8) reconstruction on the front side of the crystal. Conversely, the broad band, not present in the spectrum shown in Fig. 2c, is probably due to arsine adsorption on the back side of the crystal.

The three peaks at 2165, 2140, and 2080 cm^{-1} are attributable to As-H stretching vibrations [2,27,30,31]. Gallium hydride stretching vibrations, which occur between 1900 and 1700 cm^{-1}, are not observed in the infrared spectra. Furthermore, the As-H vibrations are indicative of the dissociative adsorption of arsine. Molecularly adsorbed arsine would exhibit a pair of closely spaced asymmetric and symmetric stretching vibrations with dipole moments oriented in opposing directions [2,30,31]. All three peaks are highly s-polarized, indicating their dipole moments are oriented along the [$\bar{1}$10] crystal axis. These results are consistent with arsine dissociatively adsorbing onto second-layer Ga atoms, and transferring its H atoms to neighboring As dimer sites. The most likely adsorbate structures are discussed in the next section.

At saturation coverage of arsine, the intensities of the As-H stretching vibrations are small. The integrated areas of the infrared bands are approximately 15% of the integrated areas of the As-H infrared bands generated upon hydrogen atom adsorption on c(2×8) GaAs(001) [28]. We estimate that at saturation coverage of hydrogen, one H atom is bonded to each As atom in the top layer, or there are six H per (2×4) unit cell [28]. Assuming that the molecular absorption coefficients for the As-H stretching vibrations of adsorbed arsine and hydrogen are the same, the intensity difference suggests that the saturation uptake of arsine molecules at 303 K is about one for every three (2×4) unit cells. This corresponds to a coverage of 0.042 ML, where 1.0 ML = 6.26×10^{14} atoms/cm^2.

Shown in Fig. 3a are polarized reflectance spectra for a saturation coverage of arsine on (1×6) GaAs(001) at 303 K. A series of As-H stretching vibrations is observed at 2135, 2100, 2045, and 2020 cm^{-1}. These bands are more intense in the s-polarized spectrum than in the p-polarized spectrum. Fig. 3b shows the arsine absorption spectrum without polarization. Fig. 3c shows the unpolarized reflectance spectrum for deuterium titration of the arsine adsorbed on the front side of the crystal. The same four As-H vibrational bands are seen, except that their intensity is half that recorded in the unpolarized spectrum. This suggests that about half the intensity in the unpolarized spectrum is due to AsH_3 adsorbed on the (1×6) surface on the front side of the crystal. The other half of the unpolarized spectral intensity may be ascribed to AsH_3 adsorbed on the back side of the crystal.

The occurrence of four distinct As-H vibrations

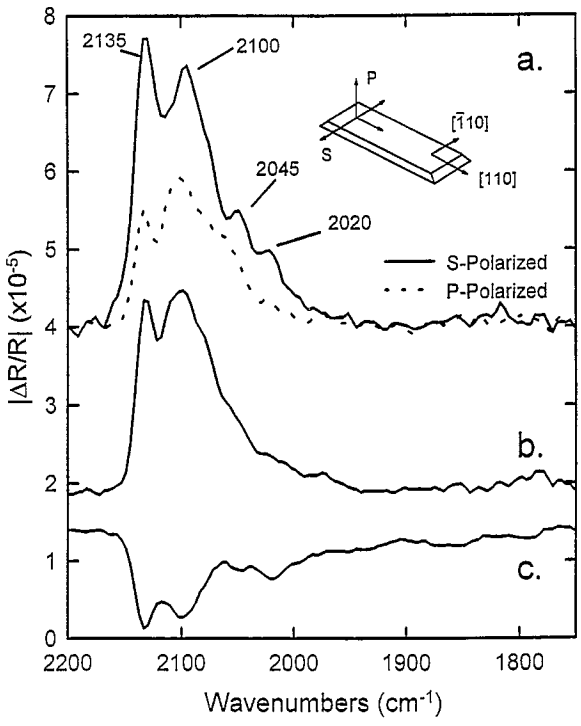

Fig. 3. Infrared reflectance spectra of adsorbed arsine on (1×6) GaAs(001) at 303 K: (a) s- and p-polarized spectra (inset diagram reveals crystal orientation); (b) unpolarized spectrum; and (c) unpolarized spectrum after deuterium titration of the adsorbed arsine.

must mean that the arsine molecules dissociate into several AsH_2 and/or AsH species on the (1×6) surface. Since the infrared bands are predominately s-polarized, the As-H bonds of these species are oriented along the $[\bar{1}10]$ axis. This is consistent with the arsine bonding to exposed gallium atoms, either at the Ga dimers, or at the second-layer Ga sites. Further inspection of Fig. 3 reveals that there are no terminal Ga-H stretching vibrations between 1900 and 1700 cm^{-1}, and no bridging Ga-H-Ga vibrations between 1700 and 1200 cm^{-1} [27]. Therefore, on both the $c(2 \times 8)$ and (1×6) surfaces, dissociative adsorption of AsH_3 occurs with the transfer of H atoms to As sites, not to Ga sites.

Comparison of Fig. 3 with Fig. 2 reveals that the intensity of the reflectance spectrum of adsorbed arsine is greater for the (1×6) than for the $c(2 \times 8)$. Evidently, the arsine uptake on the (1×6) is higher as a result of there being more exposed gallium atoms on this reconstruction. An approximate value of the adsorbate density may be obtained by comparing the intensity of the infrared bands of adsorbed arsine to those of adsorbed hydrogen [28]. In the latter case, we estimate that six H atoms are bonded to the exposed As atoms in each (2×6) unit cell at saturation coverage (1 H per As dimer atom and 1/2 H per second-layer As atom) [28]. The ratio of the integrated areas of the As-H bands for adsorbed arsine to those for adsorbed hydrogen is close to 0.5, which suggests that a maximum of one AsH_3 molecule is adsorbed per (2×6) unit cell at 303 K. This corresponds to a coverage of 0.083 ML, which is double that observed on the $c(2 \times 8)$ surface.

3.2. *Arsine adsorption at elevated temperatures*

Presented in Fig. 4 is a series of unpolarized reflectance spectra taken following arsine adsorption on $c(2 \times 8)$ GaAs(001) at elevated temperatures. In this experiment, the crystal was heated to a specified temperature between 303 and 438 K and dosed with 5×10^{-7} Torr of AsH_3 until saturation coverage (about 1 h). Single-beam spectra were collected before and during dosing at the same temperature, and ratioed to one another to give the reflectance spectra shown in the figure. At

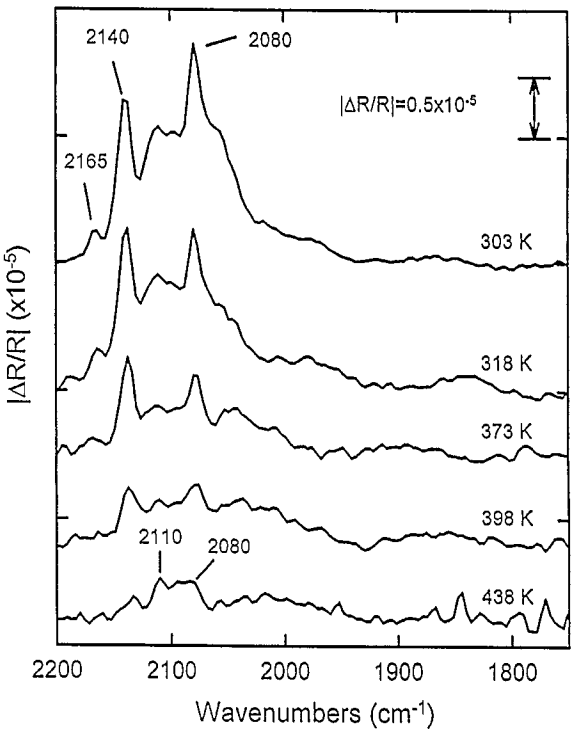

Fig. 4. Unpolarized reflectance spectra for saturation coverages of arsine on $c(2 \times 8)$ GaAs(001) at different temperatures.

303 K, three peaks are observed at 2165, 2140, and 2080 cm^{-1}. The intensities of these peaks gradually declines as the temperature is increased, such that by 438 K two very small bands remain at 2110 and 2080 cm^{-1}. These bands are similar to those observed for hydrogen adsorption on As sites on the $c(2 \times 8)$ at 438 K [28]. These data suggest that the arsine uptake decreases with increasing adsorption temperature due to its recombinative desorption. However, at 438 K a small quantity of adsorbed AsH_3 may completely decompose, causing some H atoms to become bound to As sites. It is noted that hydride transfer does not occur to the Ga sites, since no Ga-H vibrations are detected at any adsorption temperature.

When the $c(2 \times 8)$ GaAs(001) surface is dosed with 5×10^{-7} Torr AsH_3 for 1 h at 363–673 K, and held at the same temperature for 0.5 h, no change in the $c(2 \times 8)$ LEED pattern is observed. However, the As/Ga $2p_{3/2}$ area ratio increases from 1.60 to 1.68. These results may mean that the AsH_3 exposure slightly increases the As coverage, or it induces

a transformation of the (2×4) unit cells from one structure to another, such as from the $\beta2(2\times4)$ to the $\beta(2\times4)$ (refer to Fig. 1). On the other hand, when the $c(2\times8)$ is dosed with 5×10^{-7} Torr AsH_3 above 673 K, the As coverage starts decreasing, as evidenced by a drop in the XPS As/Ga area ratio and by the disappearance of the LEED pattern. These same changes occur if the sample is heated to high temperatures without any background pressure of arsine. Evidently, the rate of arsine adsorption and decomposition in 5×10^{-7} Torr AsH_3 is slower than the rate of As desorption from GaAs(001) above 673 K.

No matter how long we dosed at 363–673 K, the As coverage never exceeded 0.75, and always retained the $c(2\times8)$ reconstruction. By contrast, Banse and Creighton [15] were able to achieve arsenic coverages as high as 1.7 ML by dosing the crystal with AsH_3 at 623 K. The difference between their study and ours must lie in the flux of arsine to the surface. We exposed the crystal to 5×10^{-7} Torr of AsH_3, whereas they used AsH_3 pressures ranging from 1×10^{-5} to 3×10^{-3} Torr.

Shown in Fig. 5 are unpolarized reflectance spectra for arsine adsorption on (1×6) GaAs(001) at temperatures between 303 and 473 K. These

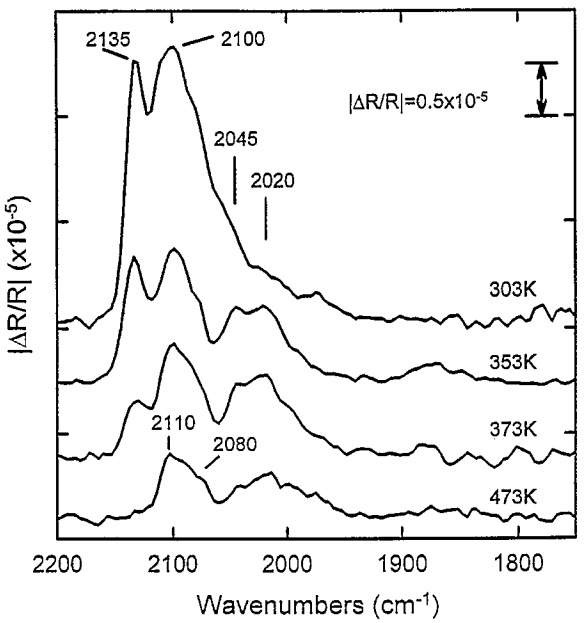

Fig. 5. Unpolarized reflectance spectra for saturation coverages of arsine on (1×6) GaAs(001) at different temperatures.

experiments were conducted in the same way as those described above for the $c(2\times8)$ surface. The intensities of the As-H stretching vibrations decrease as the crystal is heated to higher temperatures. The band at 2135 cm^{-1} declines more rapidly than the other features, and is completely gone by 473 K. It is noteworthy that at 473 K the reflectance spectrum for adsorbed arsine on the (1×6) is very similar in shape and intensity to the reflectance spectrum for adsorbed hydrogen on the $c(2\times8)$ [28]. We have previously attributed the bands at 2045 and 2020 cm^{-1} to hydrides bound to As dimer sites, and the band at 2100 cm^{-1} to hydrides bound to second-layer As atoms [27,28]. Therefore, the data in Fig. 5 suggest that arsine decomposes on the exposed Ga atoms on the (1×6) and produces As sites similar to those found on the $c(2\times8)$.

Further insight into the arsine decomposition process on (1×6) GaAs(001) can be obtained by characterizing the composition of the surface by XPS and infrared spectroscopy of adsorbed hydrogen after arsine exposure. This experiment was conducted as follows. The GaAs sample was heated to a specific temperature between 303 and 573 K, dosed with 5×10^{-7} Torr of AsH_3 for 1 h, held in vacuum at the same temperature for 0.5 h, and cooled to 303 K. An XPS spectrum was taken next. Then, a series of infrared spectra was recorded before and during dosing of the surface with H atoms. The distribution of bands in the infrared spectra reveals the distribution of adsorption sites on the surface after the AsH_3 treatment [27,28]. Deuterium titration could also have been used for this purpose. However, the deuteride vibrations are shifted to lower frequency, and one of the important infrared bands is located below the cut-off frequency of the CaF_2 windows.

Shown in Fig. 6 is a series of reflectance spectra for hydrogen titration of (1×6) GaAs(001) after dosing with arsine at different temperatures. Also shown are the As/Ga $2p_{3/2}$ area ratios recorded by XPS. The spectrum shown in Fig. 6a is of adsorbed hydrogen on the (1×6) surface precovered by AsH_3 at 303 K. This spectrum is the same as that of adsorbed hydrogen on the bare (1×6) surface, indicating that the H atoms displace all of the adsorbed AsH_3. Four main bands are seen corre-

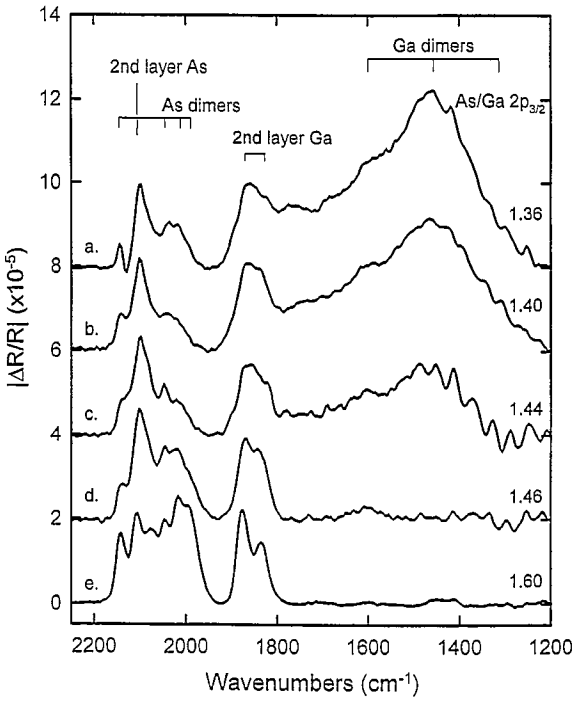

Fig. 6. Infrared reflectance spectra for hydrogen titration of (1×6) GaAs(001) after exposure to 1800 L AsH_3 at (a) 303 K, (b) 373 K, (c) 433 K, (d) 523 K, and (e) 573 K.

sponding to the four sites on this surface [27]: the peak at 2140 cm^{-1} and the doublet at 2045 and 2020 cm^{-1} are due to hydrogen adsorption on As dimers; the peak at 2110 cm^{-1} is due to hydrogen adsorption on second-layer As atoms; the band between 1950 and 1800 cm^{-1} is due to terminal gallium hydrides formed by hydrogen adsorption on second-layer Ga atoms and on Ga dimers; and the extremely broad and intense band, extending from 1800 to 1200 cm^{-1}, is due to bridging gallium hydride formed by hydrogen adsorption on Ga dimers. The vibrational data are consistent with STM images of the (1×6) [19]. As shown in the model in Fig. 1, the (2×6) unit cell contains two As dimers, two Ga dimers, four second-layer As atoms, and four second-layer Ga atoms.

Spectra presented in Fig. 6b, c, d, and e reveal the changes which occur in the distribution of surface sites due to exposing the (1×6) to AsH_3 at 373, 433, 523, and 573 K. Little change in the spectrum occurs following AsH_3 dosing at 373 K. However, starting with the treatment at 433 K, the broad, low-frequency band due to H adsorbed on Ga dimers begins to disappear, while the peaks at 2140, 2045, and 2020 cm^{-1} due to H adsorbed on As dimers begin to grow. There is also a significant increase in the XPS As/Ga area ratio from 1.30 to 1.44. After dosing with arsine at 523 K, the Ga dimer sites are completely gone and a substantial increase in the As dimer sites has occurred. Finally, when the (1×6) is exposed to arsine at 573 K, the surface is completely transformed into the $c(2\times8)$ structure. This was confirmed by LEED after the sample was cooled. Also, the spectrum shown in Fig. 6e and the XPS area ratio of 1.6 are characteristic of the $c(2\times8)$ surface. These results demonstrate that arsine decomposes on the Ga dimers exposed on the (1×6) surface and replaces them with As dimers. At 573 K, where there is sufficient mobility of the As and Ga atoms, this reaction converts the (1×6) into the $c(2\times8)$ structure.

4. Discussion

4.1. Arsine adsorption sites on $c(2\times8)$ GaAs(001)

The three narrow bands seen in Fig. 2 for arsine adsorption on $c(2\times8)$ GaAs(001) are most likely due to arsenic monohydride stretching vibrations. The formation of an arsenic dihydride can be ruled out because this species would produce asymmetric and symmetric vibrations, in which the dipole moments of these modes are orthogonal to one another. For example, Chabal and Raghavachari [32] have shown that SiH_2 groups on Si(100) exhibit asymmetric and symmetric stretches at 2104 and 2091 cm^{-1}. The former mode is parallel to the surface and exhibits mixed s- and p-polarization, while the latter mode is perpendicular to the surface and is entirely p-polarized. If one assumes that each arsine molecule forms an AsH_2 group that bridge bonds to two second-layer Ga atoms, the asymmetric mode would be strictly s-polarized, while the symmetric mode would be strictly p-polarized. As is evident in Fig. 2, the bands at 2165, 2140, and 2080 cm^{-1} are all s-polarized. The formation of a coupled monohydride, H-AsAs-H, across an As dimer, can be ruled out for the same reason. Chabal and Raghavachari

[33] have shown that coupled Si monohydrides produce asymmetric and symmetric stretches that are oriented parallel and perpendicular to the surface. It might be argued that the symmetric modes of AsH_2 and As_2H_2 groups on GaAs(001) are very weak and not easily identified in the infrared spectra. However, in the case of SiH_2 and Si_2H_2 on Si(100), the symmetric modes are observed to be more intense than the asymmetric modes. Therefore, we conclude that the bands at 2165, 2140, and 2080 cm^{-1} are due to the stretching vibrations of isolated arsenic monohydrides.

The formation of only arsenic monohydrides on the c(2×8) surface indicates that, at 303–438 K, the arsine molecules dissociatively adsorb as AsH species, and transfer two H atoms each to neighboring As dimers. A model of the adsorbate structure is shown in Fig. 7a. The model depicts the AsH_3 molecule bonding to second-layer Ga atoms on the $\beta(2\times4)$ surface. Two distinctly different hydrides are produced by this reaction: H bonded to As atoms containing unshared pairs of electrons, and H bonded to As dimer atoms. This adsorbate structure is consistent with the infrared spectrum. When the lone pair of electrons on As is replaced with a bond to another atom, the As-H bond contracts, causing its vibrational frequency to shift upwards [34–36]. For example, in the TMGa-AsH_3 adduct, the As-H stretches are approximately 40 cm^{-1} higher than those in AsH_3 [37].

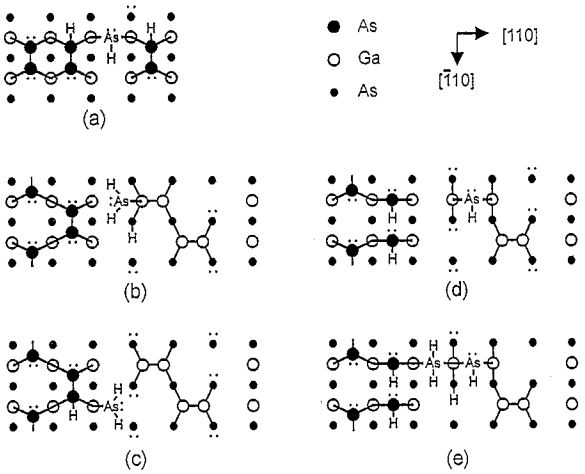

Fig. 7. Ball-and-stick models of adsorbed arsine on (a) $\beta(2\times4)$ and (b–d) (2×6) GaAs(001) at 303 K.

Accordingly, the 2080 cm^{-1} peak may be assigned to H bonded to As atoms with lone pairs, while the peaks at 2165 and 2140 cm^{-1} may be assigned to H bonded to As dimer atoms. The two high-frequency peaks could be due to As hydrides formed at different locations on the surface, such as at terraces versus at steps. On miscut Si(100) surfaces, a wide range of frequencies are observed for the hydrides bound to the steps [38]. Another feature of the model in Fig. 7a, which is consistent with the vibrational data, is the orientation of the As-H bonds. They are all aligned along the [1̄10] crystal axis, in agreement with the detection of only s-polarized infrared bands.

With regard to the $\beta2(2\times4)$ (Fig. 1), we cannot conceive of an adsorbate structure that is consistent with the infrared spectrum. On this surface an arsenic monohydride would probably bond to two second-layer Ga atoms contained in the same row (along the [1̄10] direction). This would orient the As-H bond parallel to the [110] crystal axis, yielding a p-polarized infrared band. Evidently, the c(2×8) surface prepared in this study is comprised of $\beta(2\times4)$ unit cells, or arsine adsorption induces the transformation of the $\beta2(2\times4)$ phase into the $\beta(2\times4)$.

It is significant that the infrared spectra of adsorbed arsine on c(2×8) GaAs(001) do not exhibit any Ga-H stretching vibrations. This is not because all the second-layer Ga atoms are coordinated to adsorbed As. At saturation, the As coverage is ~0.04 ML, whereas the density of Ga sites is around 0.25 ML. Nor is the absence of Ga-H bonds due to a lack of reactivity of the second-layer Ga atoms. In our study of hydrogen adsorption on GaAs(001), we found that these sites are the first ones to be occupied upon exposing the surface to a flux of H atoms [28]. We believe the reason H atoms do not transfer from adsorbed arsine to the Ga atoms is that this reaction does not conserve valence electrons. It is our hypothesis that, on gallium arsenide, the number of valence electrons is conserved in surface reactions [29]. This hypothesis is really an extension of Pashley's electron-counting model [26], because any reaction with GaAs(001) which does not maintain a constant number of valence electrons will result in

the build up of charge on the semiconductor surface.

The adsorbate model shown in Fig. 7a conserves valence electrons. The incoming AsH_3 molecule has eight electrons, and the two As atoms on the dimers have two electrons each, for a total of 12 valence electrons. This is exactly balanced by the 12 valence electrons used by the adsorbates: eight electrons for AsH bonded to the second-layer Ga atoms, and four electrons for the two hydride bonds to the As dimers. Now consider the alternative reaction where the hydrogen is transferred to gallium sites. The incoming AsH_3H molecule has eight electrons, and since the Ga dangling orbitals are empty, a total of eight electrons are available from the reactants. However, the products require 12 electrons: eight electrons for AsH bonded to the second-layer Ga atoms, and four electrons for the two hydride bonds to Ga atoms. This explains why no Ga-H infrared bands are detected. If the arsine molecule dissociatively adsorbs onto Ga atoms, then there are no valence electrons available to make gallium hydride bonds.

The absence of any Ga-H bands in the infrared spectra of adsorbed AsH_3 (Figs. 2–5) contradicts an earlier study of arsine decomposition on (4×6) GaAs(001) by Wolf et al. [14]. These authors observed a Ga-H band at 1870 cm^{-1} in a high-resolution electron-energy-loss spectrum after adsorbing arsine at 115 K and annealing the crystal between 300 and 500 K. One possible explanation for this discrepancy is that their (4×6) surface contained (4×2) domains that are comprised entirely of Ga dimers and second-layer As atoms. On these domains, H atoms may transfer to Ga sites upon the dissociative adsorption of arsine. By contrast, both the $c(2\times8)$ and (1×6) surfaces contain As dimers, and when arsine dissociates on these surfaces, the preferred equilibrium configuration is with all the H atoms transferred to As dimer sites. Another possible explanation for the discrepancy between the two studies is that in Wolf's experiments hot filaments may have been on in the chamber during dosing and annealing (such as the one on the HREELS spectrometer). The hot filaments may have dissociated arsine or hydrogen in the UHV chamber and caused H atoms to adsorb onto the gallium atoms.

4.2. Arsine adsorption sites on (1×6) GaAs(001)

The infrared spectra shown in Figs. 3 and 5 of arsine adsorbed on (1×6) GaAs(001) contain a series of overlapping bands due to As-H stretching vibrations. Most of these bands appear to be strongly s-polarized, although the degree of polarization is hard to assess due to the contribution to the spectra of the arsine adsorbed on the back face of the crystal. Nevertheless, these data indicate that arsine molecules dissociatively adsorb onto (1×6) GaAs(001), and transfer one or two of their H atoms to nearby As sites. Potential adsorbate structures are shown in Figs. 7b–7e. We tend to favor the formation of monohydrides (Fig. 7d) over dihydrides (Figs. 7b, 7c, and 7e) because the former structure is consistent with the highly s-polarized stretching vibrations. In addition, the model in Fig. 7d is analogous to the structure we have proposed for the $c(2\times8)$ surface. We cannot, however, rule out the AsH_2 structures, since there is sufficient p-polarized intensity in the vibrational spectrum to justify the existence of the symmetric stretching mode for this species.

The model in Fig. 7d is also in good agreement with the experimental results obtained from dosing the (1×6) with arsine at elevated temperatures. The infrared spectra collected at 353–473 K (Fig. 5) contain prominent bands at approximately 2135, 2045, and 2020 cm^{-1}. These features are seen in the infrared spectra of hydrogen adsorbed on the (1×6) and $c(2\times8)$ surfaces (see Fig. 6a and e), and are attributed to H atom adsorption on As dimers. Furthermore, when the (1×6) surface is titrated with hydrogen after arsine adsorption at 433–573 K, we find that the Ga dimer sites are progressively replaced by "As dimer-like" adsorption sites. Insertion of the arsine molecule across the Ga dimer bond, as depicted in the model in Fig. 7d, is clearly the most logical way for As to remove the Ga dimers from the surface.

The arsine coverages shown in the models in Fig. 7 corresponds to one molecule per (2×4) unit cell, or 0.125 ML, and one molecule per (2×6) unit cell, or 0.083 ML. Inspection of the drawings reveals that these values are half that theoretically possible: one AsH_3 molecule should be able to dissociatively adsorb onto every two second-layer

Ga atoms on the (2×4) and onto every Ga dimer on the (2×6). However, lower coverages are estimated from the integrated intensities of the As-H bands at 303 K. The saturation uptakes are found to be 0.042 and 0.083 ML for the $c(2\times8)$ and (1×6) surfaces, respectively. The reason the coverages are lower than their maximum values is most likely due to the recombinative desorption of some of the arsine at 303 K. Bansenauer and Creighton [16] have shown that this reaction occurs at temperatures as low as 250 K on the $c(2\times8)$ and (4×6) surfaces.

4.3. Arsine decomposition mechanism on GaAs(001)

Before proposing a mechanism, it is useful to review the results already in the literature for arsine decomposition on GaAs(001). Several authors [13–16] have investigated the thermal desorption of arsine and its decomposition products from the (4×6), $c(2\times8)$, and $c(4\times4)$ reconstructions. In these studies, AsD_3 was adsorbed to saturation coverage at about 115 K, then the crystal surface was heated at 5 K/s and the desorption products measured with a mass spectrometer. It was found that most of the arsine desorbs from the (4×6) in three bursts at 165, 290, and 380 K, whereas on the $c(2\times8)$, arsine desorbs in a series of bursts at 165, 235, 375, and 460 K. In both cases, the lowest temperature peak was ascribed to the desorption of molecularly bonded arsine, while the higher temperature peaks were assigned to the recombinative desorption of dissociatively adsorbed arsine. The amount of arsine desorbing was estimated at 0.09 ML from the (4×6) and 0.18 ML from the $c(2\times8)$. During heating, a very small amount of AsD_3, $\sim$ 0.01 ML, decomposes on these surfaces with the desorption of D_2. The D_2 peaks are observed at 520 K for the (4×6) and 600 K for the $c(2\times8)$. Thermal desorption of arsine from the $c(4\times4)$ occurs in a single burst at 165 K. No dissociation or decomposition of AsD_3 is recorded on this surface.

In another study, Banse and Creighton [15] exposed a gallium-rich GaAs(001) surface to large doses of arsine at 623 K, and they observed the deposition of up to 1.7 ML of As atoms. Upon flashing the crystal to 900 K, the arsenic desorbs from the surface in three peaks located at 713, 753, and 843 K. The peak at 713 K is due to As_4 desorption from surfaces covered with 1.75–1.00 ML As, while the peaks at 753 and 843 K are due to As_2 desorption from surfaces covered with 1.00–0.75 ML As, and with 0.75–0.25 ML As, respectively. With decreasing arsenic coverage, the GaAs(001) surface undergoes several phase transitions from $c(4\times4)$ at 1.75 ML As to $c(2\times8)$ at 0.75 ML As to $c(8\times2)$ at 0.25 ML As. The occurrence of three peaks in the TPD spectrum is related to these changes in the surface structure. The first two lower temperature peaks result from As_4 and As_2 desorption from double-dimer sites, i.e., to sites in which the As dimers in the top layer are bonded to a full layer of As atoms underneath. By contrast, the high temperature peak is due to As_2 desorption from As dimers that are bonded to a layer of Ga atoms. Arsenic bonded to gallium is more strongly held than arsenic bonded to arsenic, and so more energy is required to desorb it.

Based on the preceding results, the following sequence of steps may be proposed for arsine decomposition on GaAs(001):

$$AsH_3 + 3^* \rightleftarrows {}^*AsH + 2^*H, \tag{4}$$

$${}^*AsH + {}^* \rightarrow {}^*As + {}^*H, \tag{5}$$

$$2^*H \rightarrow H_2 + 2^*, \tag{6}$$

$${}^*Ga + {}^*As \rightarrow GaAs_s + 2^*, \tag{7}$$

$$2^*As \rightleftarrows As_2 + 2^*, \tag{8}$$

$$4^*As \rightleftarrows As_4 + 4^*, \tag{9}$$

where * is a surface site. This mechanism has been written in the simplest way possible to illustrate the main steps in the process. Some of the reactions obviously represent the sum of several elementary steps. Under OMVPE or ALE reaction conditions, we anticipate that dissociative adsorption of arsine is fast and equilibrated. Hydrogen desorption is also fast, so that the H coverage under the reaction conditions is probably low. The slowest steps in the process are the desorption of As_2 and As_4. The arsine consumption rate is determined by the rate of H_2 desorption (reaction (6)) relative to the rate of recombinative desorption of AsH_3 (reverse of

reaction (4)). The arsine selectivity to film growth is determined by the rate of reaction of adsorbed As and Ga (reaction (7)) relative to the rates of desorption of arsenic (reactions (8) and (9)).

The role played by the surface in the decomposition reaction is one of the interesting parts of this story. Our infrared study has revealed that arsine dissociatively adsorbs onto two different sites on the GaAs(001) surface: second-layer Ga atoms and Ga dimers. In both cases, the H atoms are transferred to neighboring arsenic sites, most likely these sites being the As dimers. We find that at 303 K, the arsine uptake on the (1×6) surface is twice that on the $c(2\times8)$, indicating that adsorption on Ga dimers is favored over adsorption on second-layer Ga atoms. This may be contrasted with the observation by Bansenauer and Creighton [16] that the arsine uptake on the $c(2\times8)$ is twice that on the (4×6). The reason for this may be that the (4×6) does not contain a sufficient number of exposed As atoms (or As dimers) to transfer the H atoms upon arsine dissociation. With regard to the decomposition of the adsorbed arsine, we know that this occurs on both the second-layer Ga atoms (i.e., $c(2\times8)$ surfaces) and the Ga dimers (i.e., (1×6) and (4×6) surfaces), since it has been shown that up to 1.7 ML As may be deposited on GaAs(001) by exposure to AsH_3 at 623 K [15]. However, there is an important distinction between these two sites: arsine decomposition on Ga dimers directly leads to As incorporation into the crystal lattice (as documented in Fig. 6), whereas on the second-layer Ga sites, there does not appear to be a direct pathway for As incorporation.

Shown in Fig. 8 is a site-specific mechanism for arsine decomposition on the second-layer Ga atoms on $\beta(2\times4)$ GaAs(001). The valence electrons are conserved in each reaction shown. In the first step, AsH_3 molecules adsorb onto the Ga atoms and sequentially dissociate into arsenic monohydrides. Two molecules are shown sticking to the Ga sites to give the maximum theoretical coverage. Hydrogen desorption occurs next, leading to the formation of a fourth As dimer. One hydride remains bound to each As dimer after this reaction. In depicting the reaction this way, we do not imply that H_2 desorption and As dimerization have to occur in a concerted fashion. Desorption

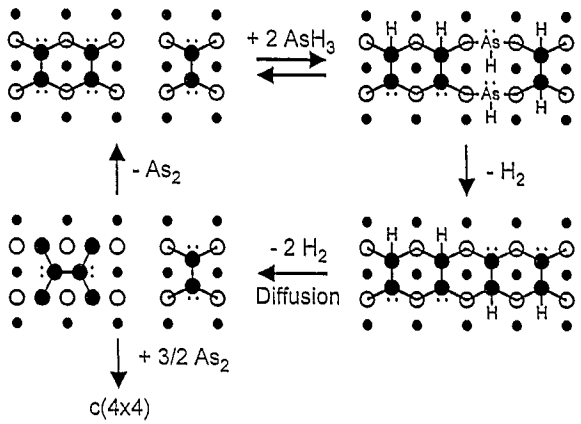

Fig. 8. Ball-and-stick model of arsine decomposition on $\beta(2\times4)$ GaAs(001).

could take place first, followed by diffusion of As atoms along the vacancy rows, and then dimerization. Banse and Creighton [15] have observed a $(2\times1)+1/2n$X* LEED pattern after exposing GaAs to 4.0×10^5 L AsH_3 at 548 K. The continuous row of hydrogenated As dimers could be responsible for this structure. However, further experiments are necessary to confirm this.

In the third step shown in Fig. 8, the remaining hydrogen desorbs from the surface, leaving behind two additional As atoms. In order for these atoms to be covalently bound in a way that does not accumulate excess charge on the surface, they must migrate to the As dimers and form a double-dimer structure. In the following step, the As dimer may desorb as As_2 and regenerate the $\beta(2\times4)$ surface. Alternatively, more As dimers can accumulate from AsH_3 decomposition, causing the $c(4\times4)$ phase to nucleate and spread across the surface [15,39–41]. The four basic steps illustrated in the figure are clearly documented by the experimental results described above.

Presented in Fig. 9 is a model for arsine decomposition on the Ga dimers on (2×6) GaAs(001). Arsine adsorbs on the Ga dimers, then dissociates and inserts across the Ga dimer bond, forming an arsenic monohydride. Hydrogen atoms are transferred to adjacent As dimers during this reaction. In the second and third steps, H_2 molecules are sequentially desorbed from the surface. Under a continuous flux of arsine at $\geqslant$573 K, hydrogen desorption will be accompanied by diffusion of As

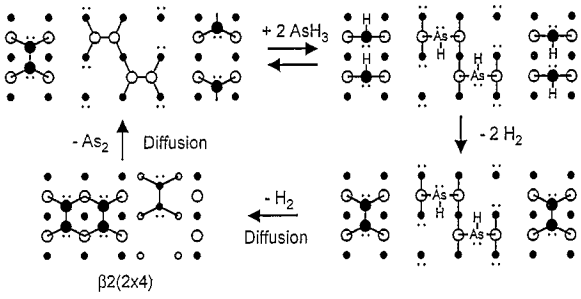

Fig. 9. Ball-and-stick model of arsine decomposition on (2×6) GaAs(001).

and Ga atoms across the surface, and the transformation of the (2×6) into the (2×4) reconstruction. This transformation was observed in our experiments (refer to Fig. 6, spectrum e). On the other hand, in the absence of an arsine flux, the arsenic can desorb as As_2 and regenerate the (2×6) surface.

Under OMVPE growth conditions, it may be that there is no long range order giving rise to a discernible reconstruction. Nevertheless, the GaAs(001) surface is still terminated with As and Ga dimers [39–43]. Therefore, the models presented in Figs. 8 and 9 ought to be viewed as representing reactions which occur on specific sites. These sites may be distributed randomly over the surface during film growth. Comparison of Figs. 8 and 9 reveals that if the arsine adsorbs and decomposes on a Ga dimer, it can incorporate into the crystal and contribute to film growth. If, on the other hand, the arsine adsorbs and decomposes on a second-layer Ga atom, it most likely will be transferred to As sites and then desorb as As_2 or As_4.

5. Conclusions

In this paper we have shown that arsine adsorbs onto two sites on GaAs(001) surfaces: second-layer Ga atoms and Ga dimers. At 303 K, arsine dissociatively adsorbs as an arsenic monohydride, and transfers its H atoms to nearby As sites. Under no circumstances is hydride transfer to gallium observed. Above 473 K, arsine will decompose on both second-layer Ga atoms and Ga dimers with the desorption of H_2 from the surface. We find that exposing the $c(2\times8)$ to 5×10^{-7} Torr of AsH_3 at 573 K leads to no change in the composition or structure of the surface. However, exposing the (1×6) to the same arsine flux at 573 K causes it to slowly transform into the $c(2\times8)$ reconstruction. Based on these and other results, we conclude that during the vapor-phase growth of GaAs using TMGa and AsH_3, arsine decomposes on both second-layer Ga atoms and Ga dimers, but on the latter sites, the arsenic is more likely to be incorporated into the crystal.

Acknowledgements

The authors wish to thank the National Science Foundation (grant CTS-9121811) for financial support of the work, and Haluk Senkur at Rockwell for providing the arsine.

References

[1] D.H. Reep and S.K. Ghandhi, J. Electrochem. Soc. 130 (1983) 675.
[2] J. Nishizawa and T. Kurabayashi, J. Electrochem. Soc. 130 (1983) 413.
[3] J. Nishizawa and T. Kurabayashi, Vacuum 41 (1990) 319.
[4] T.F. Kuech, Mater. Sci. Rep. 2 (1987) 1.
[5] T.F. Kuech, Proc. IEEE 80 (1992) 1609.
[6] G.B. Stringfellow, Organometallic Vapor-Phase Epitaxy, Theory and Practice (Academic Press, New York, 1989).
[7] M.L. Hitchman and K.F. Jensen, Chemical Vapor Deposition (Academic Press, San Diego, CA, 1993).
[8] T.F. Kuech and E. Veuhoff, J. Cryst. Growth 68 (1984) 148.
[9] J.R. Creighton, B.A. Bansenauer, T. Huett and J.M. White, J. Vac. Sci. Technol. A 11 (1993) 876.
[10] K. Tamaru, J. Phys. Chem. 59 (1955) 777.
[11] M.R. Leys and H. Veenvliet, J. Cryst. Growth 55 (1981) 145.
[12] C.A. Larsen, N.I. Buchanan and G.B. Stringfellow, Appl. Phys. Lett. 52 (1988) 480.
[13] X.-Y. Zhu, M. Wolf, T. Huett, J. Nail, B.A. Banse, J.R. Creighton and J.M. White, Appl. Phys. Lett. 60 (1992) 977.
[14] M. Wolf, X.-Y. Zhu, T. Huett and J.M. White, Surf. Sci. 275 (1992) 41.
[15] B.A. Banse and J.R. Creighton, Appl. Phys. Lett. 60 (1992) 856.

[16] B.A. Bansenauer and J.R. Creighton, Surf. Sci. 278 (1992) 317.
[17] A.J. Van Bommel, J.E. Crombeen and T.J. Oirschot, Surf. Sci. 72 (1978) 95.
[18] R.Z. Bachrach, R.S. Bauer, P. Chiaradia and G.V. Hansson, J. Vac. Sci. Technol. 19 (1981) 335.
[19] D.K. Biegelsen, R.D. Bringans, J.E. Northrup and L.E. Swartz, Phys. Rev. B 41 (1990) 5701.
[20] P.K. Larsen and D.J. Chadi, Phys. Rev. B 37 (1988) 8282.
[21] D.J. Chadi, J. Vac. Sci. Technol. A 5 (1987) 834.
[22] M.D. Pashley, K.W. Haberern, W. Friday, J.M. Woodall and P.D. Kirchner, Phys. Rev. Lett. 60 (1988) 2176.
[23] M.D. Pashley, K.W. Haberern and J.M. Gaines, Surf. Sci. 267 (1992) 153.
[24] V. Bressler-Hill, M. Wassermeier, K. Pond, R. Maboudian, G.A.D. Briggs, P.M. Petroff and W.H. Weinberg, J. Vac. Sci. Technol. B 10 (1992) 1881.
[25] J.E. Northrup and S. Froyen, Phys. Rev. B 50 (1994) 2015.
[26] M.D. Pashley, Phys. Rev. B 40 (1989) 10481.
[27] H. Qi, P.E. Gee and R.F. Hicks, Phys. Rev. Lett 72 (1994) 250.
[28] H. Qi, P.E. Gee, T. Nguyen and R.F. Hicks, Surf. Sci. 323 (1995) 6.
[29] P.E. Gee, H. Qi and R.F. Hicks, Surf. Sci. 330 (1995) 135.
[30] V.M. McConagie and H.H. Nielsen, Phys. Rev. 75 (1949) 633.
[31] D. Speckman, J. Cryst. Growth 116 (1992) 48.
[32] Y.J. Chabal and K. Raghavachari, Phys. Rev. Lett. 54 (1985) 1055.
[33] Y.J. Chabal and K. Raghavachari, Phys. Rev. Lett. 53 (1984) 282.
[34] K.D. Dobbs, M. Trachtman, C.W. Bock and A.H. Cowley, J. Phys. Chem. 94 (1990) 5210.
[35] C.W. Bock, M. Trachtman and G.J. Mains, J. Phys. Chem. 96 (1992) 3007.
[36] R.M. Graves and G.E. Scuseria, J. Chem. Phys. 96 (1992) 3723.
[37] E.A. Piocos and B.S. Ault, J. Am. Chem. Soc. 111 (1989) 8978.
[38] Y.J. Chabal, J. Vac. Sci. Technol. A 3 (1985) 1448.
[39] F.J. Lamelas, P.H. Fuoss, P. Imperatori, D.W. Kisker, G.B. Stephenson and S. Brennan, Appl. Phys. Lett. 60 (1992) 2610.
[40] F.J. Lamelas, P.H. Fuoss, D.W. Kisker, G.B. Stephenson, P. Imperatori and S. Brennan, Phys. Rev. B 49 (1994) 1957.
[41] A.P. Payne, P.H. Fuoss, D.W. Kisker, G.B. Stephenson and S. Brennan, Phys. Rev. B 49 (1994) 14427.
[42] I. Kamiya, D.E. Aspnes, H. Tanaka and R. Bhat, Phys. Rev. Lett. 68 (1992) 627.
[43] I. Kamiya, D.E. Aspnes, L.T. Florez and J.P. Harbison, Phys. Rev. B 46 (1992) 15894.